III MODERN ELECTRONIC TECHNIQUES APPLIED TO PHYSICS AND ENGINEERING

A. DESIGN AND CONSTRUCTION OF A MICROWAVE ACCELERATOR

Staff
Professor A F Kip
Dr W H Bostick
R J Debs
P T Demos
M. Labitt
L Maier
S J Mason
I Polk
J R Terrall

The several purposes of this project have been described in detail in previous progress reports In general, the project is concerned with the problems of optimum method of construction, and the determination of limitations on the size of a microwave accelerator.

Status of Construction Ten one-foot sections of the accelerating cavity are essentially finished, and the vacuum manifold for the ultimate 20-foot length is completed Two alternative power supplies for feeding the 20 magnetrons are in the final stages of construction One of these is a d-c system powered by a motor-generator set which will give a variable pulse repetition rate up to 300 cps The other is an a-c transformer system with a fixed repetition rate of 120 cps A one-foot section of accelerating cavity has been constructed with geometry suitable for an electron velocity of 0.9 the velocity of light This section will be available for use in the initial stages of the accelerator if the accelerator is completed before 2-Mev electrons are obtainable from the Van de Graff generator

Experimental Work in Progress

(1) Phasing of Magnetrons It now appears that the most convenient method of achieving proper phase relationships between the various magnetrons will be to lock them together at the beginning of each pulse by means of signals from a single prepulsed magnetron through a padded line and T-R box A number of tests have already been made on this method and we will soon be able to make final tests to demonstrate that the method is satisfactory

(2) Thoria Cathode Electron Source In view of its possible usefulness as an electron source, thoria cathodes have been made and their operation studied We have been easily able to exceed the one-ampere pulsed current needed and at the same time to get a rectilinear beam of electrons

III B ULTRASONICS RESEARCH PROGRAM

Staff: Dr. J K Galt
Dr J R Pellam
R A Rapuano
W Roth

1 Ultrasonic Measurements in Liquefied Gases

Staff: Dr. J. K Galt

The program of measuring absorption and velocity of sound in liquefied gases, especially argon, has now been completed As explained in the April 15, 1947 Progress Report the measurements are made at roughly 45 Mc (44 4 Mc) in order to obtain an attenuation which can be measured with some precision The equipment used is that described in the January 15, 1947 Progress Report in connection with measurements on liquid helium The argon, and higher-temperature oxygen runs were done in a Dewar The nitrogen hydrogen and low-temperature oxygen runs were done in a Collins cryostat

The results obtained are shown in Table I The theoretical values to be expected from the viscosity of the gases is also given The heat conductivities of these liquids are not available so that no calculation of attenuation due to this factor can be given.

TABLE I Ultrasonic Absorption and Velocities (all values are measured at 44.4 Mc).

Liquid	Temp(°K)	Velocity$_4$ in units of 10^4 cm/sec	$\alpha_{exp}(cm^{-1})$	$\alpha_{vis}(cm^{-1})$ (calc at 44.4 Mc)
Argon	85.2 ± 0.2	8.53	0.20	0.16
Oxygen	87 0 ± 0.2	9.52	0 17	0 11
	70 ± 1	10 94	0 17	0 11
	10 ± 5	11 19	0 17	0.17 at 60°K 0.12 at 65°K
Nitrogen	73 9 ± 0.2	9 62	0.21	0 13
Hydrogen	17 ± 1	11.87	0 11	0 01

The precision of the velocity readings is 1 per cent That of the attenuations in argon, hydrogen, and oxygen is 10 per cent, and that of the nitrogen attenuation is 15 per cent The purity of the samples is stated by the supplier to be as follows argon 99.8 per cent oxygen 99 5 per cent, nitrogen 99.5 per cent, hydrogen 99 5 - 99 7 per cent The impurities in the nitrogen may have influenced the velocity The values measured here agree with that of Hirschlaff[1] rather than that of Liepmann[2] The attenuation agrees closely enough with α_{vis}, however, so that any impurities do not seem to have caused a very large change in it

1 E Hirschlaff, Proc Cambr Phil Soc 34, 296 (1938)
2 H. W Liepmann, Helv. Phys Acta 11,381 (1938); 12, 421 (1939).

No variation of attenuation with temperature was observed It should be mentioned, however, that larger attenuations were often measured near the boiling point of the liquids This is attributable to the presence of bubbles and cavitation due to the ultrasonic wave itself

A magnetic field of the order of 1000 gauss was applied to the oxygen sample to see if any effect on absorption could be observed as it has been in gaseous oxygen[1] The experimental arrangement was such that a change of 1 per cent in velocity or 20 per cent in attenuation could have been observed but no variations were noted

III B 2. Elastic Constants and Attenuation in Single Crystals

Staff Dr J K Galt

The measurements on NaCl, KBr, and KCl crystals are now finished and a summary of the results will be presented here.

The room temperature elastic constants are given in Table I along with those obtained by Huntington[2] and Durand[3] The agreement with Huntington's measurements indicates the accuracy of the technique The two sets of measurements are quite independent The disagreement with Durand on c_{11} in NaCl would indicate a slight error in Durand's measurement Hunter and Siegel using the same method as Durand's have obtained a value ($4\ 86 \times 10^{11}$) in agreement with the present measurements

TABLE I. Elastic Constants Measured at Room Temperature (Units are dynes/cm^2).

	NaCl	KBr	KCl
$c_{11} \times 10^{-11}$			
Galt	4 87	3.46	3.98
Huntington	4.85	3 45	
Durand	4 99		4 00 (extrapolated to 300°K)
$c_{12} \times 10^{-11}$			
Galt	1 24	0.58	0 62
Huntington	1.23	0.54 ± 0 03	
Durand	1 31		0 6
$c_{44} \times 10^{-11}$			
Galt	1 26	0 505	0 625
Huntington	1 26	0 508	
Durand	1.27		0.631 (extrapolated to 300°K)

The measurements of the elastic constants of KBr in the low-temperature range are shown in Figs 1 and 2 The stopcock grease film and cracking which occurs in the sample at low temperatures reduce the accuracy of these measurements from that of the room temperature elastic constants, but the curves plotted are considered precise to

1 A Van Itterbeek and L Thys, Physica, Haag 5, 298 (1938)
2 H B Huntington, Phys Rev 72, 321 (1947).
3 M A Durand, Phys Rev 50, 449 (1936).

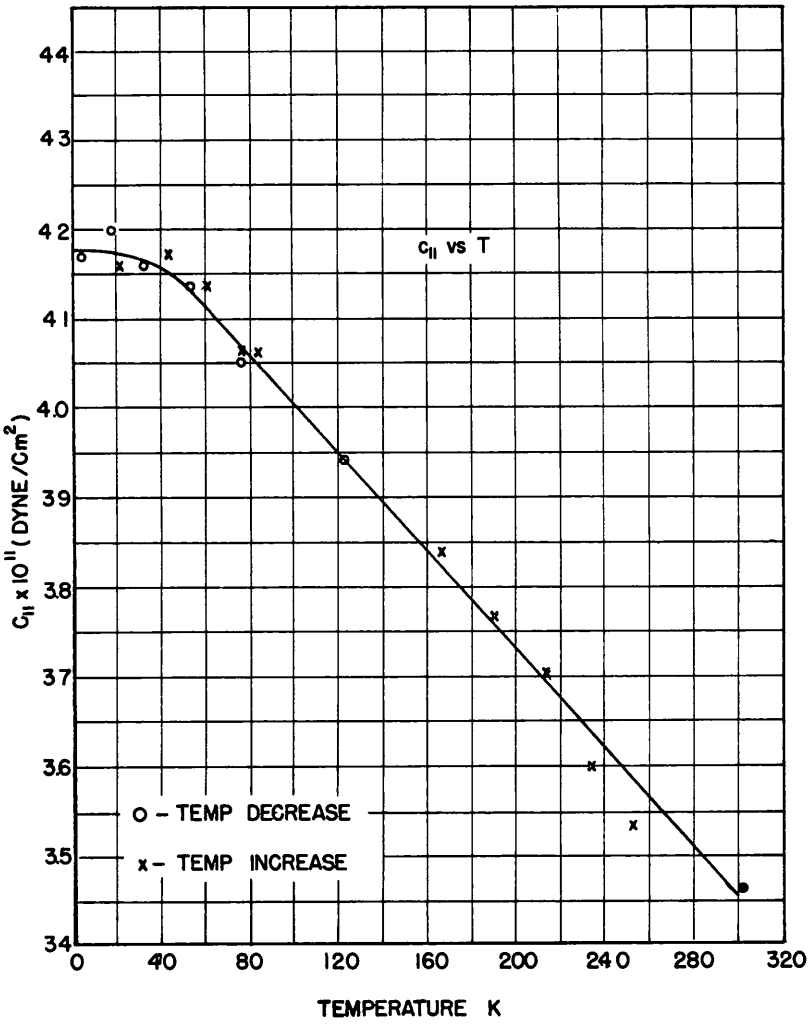

Figure 1.

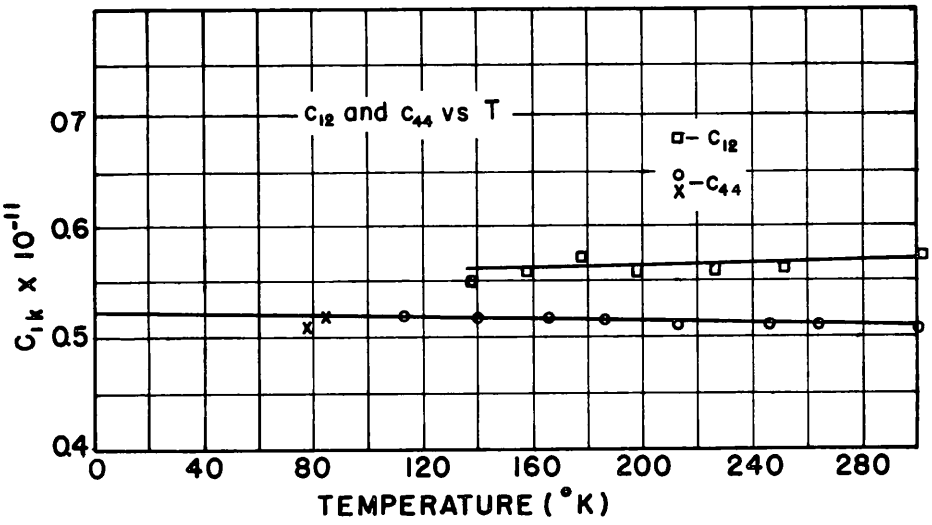

Figure 2.

within 1 per cent The cracks which occur in the sample below about 100°K are due to forces produced by the differential thermal contraction between the alkali-halide and the quartz crystal. The waves used in measuring c_{11} and c_{44} travel along the 100 direction They therefore travel parallel to the cracks, and these measurements can be made even after cracking occurs The waves used to measure c_{12} travel along the 110 direction so that when the cracks occur they break across the path of the wave and destroy the echo pattern. For this reason no measurements were obtained on c_{12} below 138°K.

The attenuations of the various waves measured are shown in Table II These values are averaged over rather long distances of travel, and the wave has in general spread out to fill the cross section of the crystal, so that the propagation conditions affect the measurements In fact, in view of the fact that no significant variation occurs among the values obtained for shear waves or among those obtained for compressional waves, it is felt that these values can only be considered upper limits and that they are to a large extent determined by propagation conditions Experience in taking the data leads to the same conclusion. The cross-sectional dimensions of the alkali-halide samples used varied by only about 10 per cent

Table II Attenuations Measured at Room Temperature

Substance	Wave		α (cm^{-1})
	Propagation direction	Shear direction	
NaCl	100	$1\bar{1}0$	0.0041
	100	010	0 0046
	100 (compressional)		0.0017
KBr	110	$1\bar{1}0$	0.0043
	100	010	0.0048
	100 (compressional)		0.0011
KCl	110	$1\bar{1}0$	0.0040
	100	010	0 0054*
	100 (compressional		0 0034*

* These values are slightly high, because the surfaces between which the wave travelled were not perfectly parallel

The optical behavior of a strained crystal is determined by the strain-optical constants (p_{ik}) of the crystal. These constants are p_{11}, p_{12}, and p_{44} in the case of cubic crystals Ratios of these constants have been determined for NaCl, KBr, KCl by measuring the change in polarization suffered by light diffracted by ultrasonic waves in crystals of these materials This is done by observing the crossed position of two polarizers with the ultrasonic wave off and comparing it with the position at which the diffracted light is crossed out The method used is that suggested by Mueller[1] (his method B).

1. H. Mueller Zeitz f Kristallographie (A) 99, 122 (1938).

The results of these measurements are shown in Table III The precision of the measurement is indicated in the table Pockels' data for NaCl and KCl, obtained by a static method, are presented for comparison

Table III Ratios of Strain-optical Constants

Substance		p_{12}/p_{11}	$p_{44}/(p_{11} + p_{12})$	p_{44}/p_{11}
NaCl	Pulsed ultrasonic measurement	1 35 $\pm$ 0.03	-0.042 $\pm$ 0 004	-0 099
	Pockels (static method)	1.30	-0 0343	-0 079
KCl	Pulsed measurement	0 76 $\pm$ 0 01	-0 069 $\pm$ 0 004	-0.12
	Pockels	0 74	-0 069	-0 12
KBr	Pulsed measurement	0 77 $\pm$ 0 01	-0 067 $\pm$ 0 005	-0 12

These results are quite consistent with the predictions of Mueller's [1] theory In particular, he predicts the agreement between the KCl and KBr values

1 H. Mueller, Phys Rev 47 947 (1935)

III B 3 Ultrasonic Absorption in Metals

Staff: W Roth

The experimental studies of ultrasonic absorption in metals in the frequency range from 5-100 Mc have been completed and a rather detailed summary is in order Of the six metals tested magnesium aluminum brass copper nickel and monel, only the first two transmit pulses in the above frequency range well enough for measuring purposes Therefore, only results for magnesium and aluminum will be discussed

Measuring Technique Figure 1 is a view of the experimental equipment as arranged for a run (A) is the electrical console containing electrical pulse generation and reception circuits suitable for pulse widths ranging from about 15 μsecs at 5 Mc to 2 μsecs at 100 Mc The plug-in coils (B), are used for band switching to provide the wide frequency coverage desired Tuning within each band is done with the calibrated dials observed on the panel Peak electrical power output of 200 watts was measured at 25 Mc

The electric r-f pulses are fed to the quartz crystal transducer mounted at the bottom of the glass test tank (C) Here, conversion to ultrasonic energy results in a longitudinal beam about 1/4 in in diameter propagating upward in a distilled water bath The metal under test is immersed in the liquid and intercepts the beam to produce patterns on the screen of the Dumont A/R Range Scope (D). Typical patterns are shown in Figs 2 and 3

Figure 2a shows echoes resulting from a homogeneous rod of fused quartz Deflection is downward and time increases to the right The first pulse at the left-hand edge of the sweep is the main bang The delay before the second pulse is due to the time of propagation in the liquid before the transmitted pulse strikes the first surface of the quartz The reflection from the first surface produces the second echo which, in this case, is of sufficient intensity to overload the receiver slightly

The train of pulses following that caused by the first surface results from multiple reflections between the two parallel surfaces of the quartz The exponential decrease in amplitude should be noted; this occurs only when materials that appear homogeneous to the beam are used Since fused quartz of the length used here 1 3/8 in., has extremely low attenuation, the absorption indicated by this exponential envelope is principally due to the reflection loss at the water-quartz interface The reflection coefficient at this boundary is not unity; hence, not all the energy continually reflects back and forth within the quartz; a fraction is lost each round trip and the exponential decay results

Figure 2b is a similar photograph showing the pattern obtained for fine-grained magnesium The only difference to be noted is the increased absorption in the metal as indicated by the increased slope of the exponential Figure 2c is the result for coarse-grained magnesium. No exponential envelope is observed because the scattering and refraction processes resulting from the non-homogeneities of the large grains introduce interference effects Thus, one pulse may be small due to phase cancellation, while the next may be large as a result of phase addition

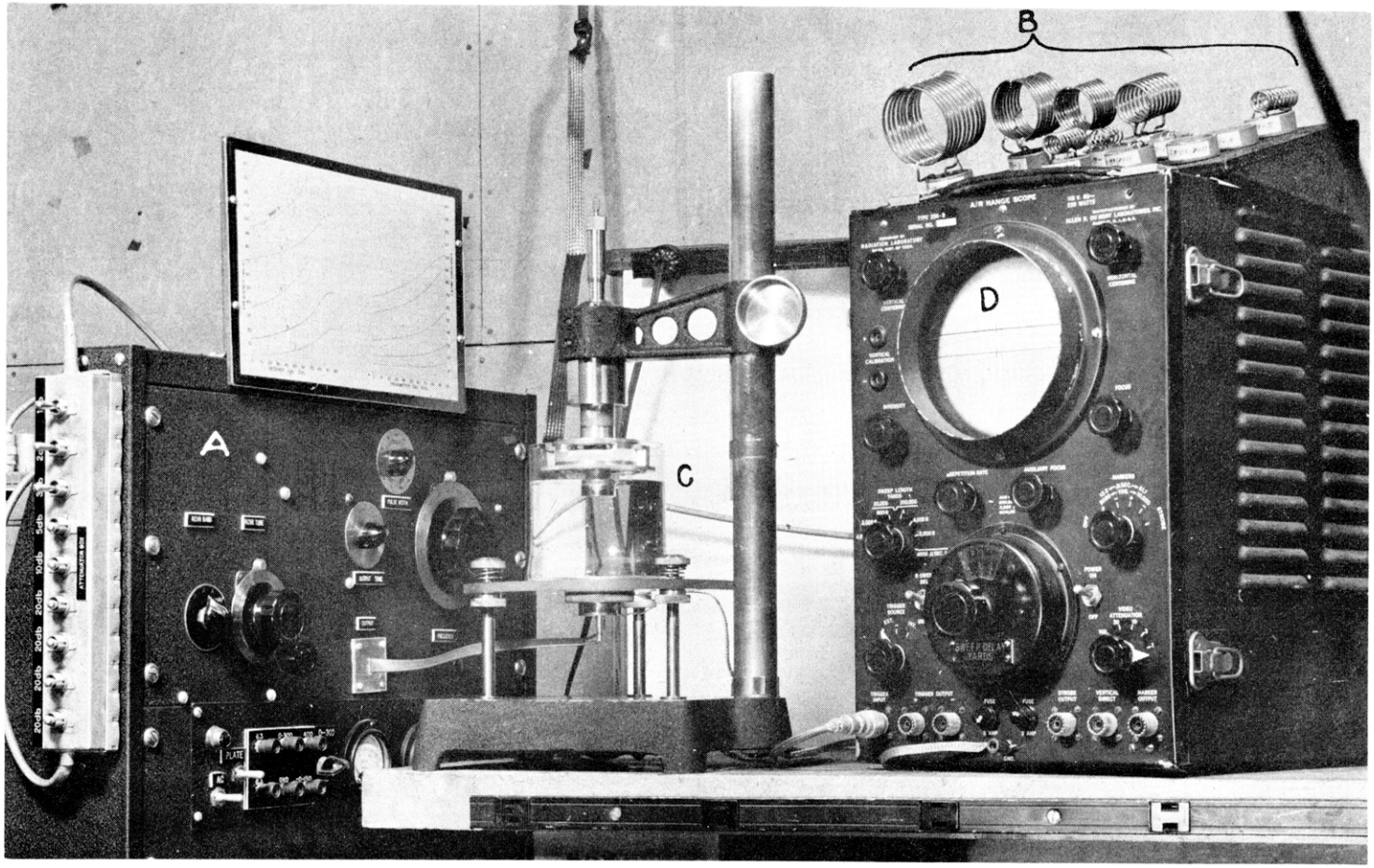

Figure 1. Arrangement of experimental equipment.

(a)

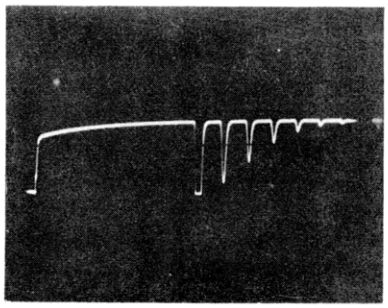

Fused quartz
diam. = ½ in.
length = 1 3/8 in.
f = 28.2 Mc/sec
pulse width = 2.5 μsec
sweep length = 122 μsec

(b)

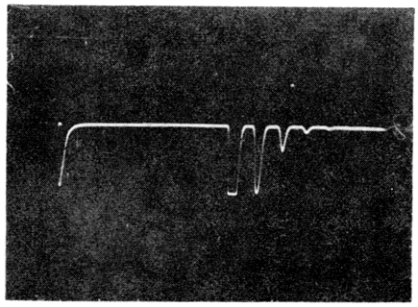

Magnesium
diam. = 1 in.
length = 1 1/4 in.
D* = 0.35 mm
f = 16.9 Mc/sec
pulse width = 3.5 μsec
sweep = 122 μsec
D/λ = 1.5

*D = grain size

(c)

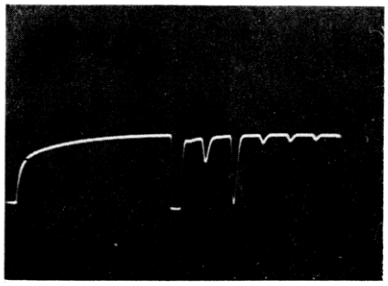

Magnesium
diam. = 1 in.
length = 1 1/4 in.
D = 1.8 mm
f = 16.9 Mc/sec
pulse width = 3.5 μsec
sweep = 122 μsec
D/λ = 7.6

(d)

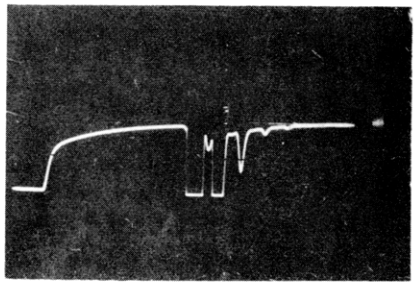

Aluminum
diam. = 3/4 in.
length = 1 ½ in.
D = 0.21 mm
f = 16.9 Mc/sec
pulse width = 3.5 μsec
sweep = 122 μsec
D/λ = 0.88

Figure 2.

Figure 2d is for aluminum and illustrates an effect previously absent, namely, energy return from metal between the surfaces. This is indicated by the hump between the second and third pulse. A more extreme case of this phenomenon is shown in Fig. 3a. The metal here is brass, although this pattern is typical of most non-homogeneous anisotropic materials. In this case, the scattered energy from the grain boundaries is large enough to mask completely the energy reflected from the surface. No measurement can be made with such a pattern. Figure 3b is exactly the same except that the pulse width is slightly greater. The general pattern is the same, but the detailed fluctuations are not. This implies that the increased length of the wave train has affected the phase relationships

(a)

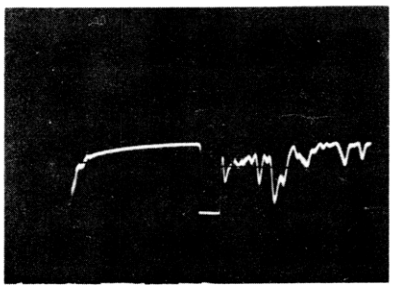

Brass (70-30)
1-in. cube
f = 16.9 Mc/sec
pulse width = 3.5 μsec
sweep = 122 μsec

(b)

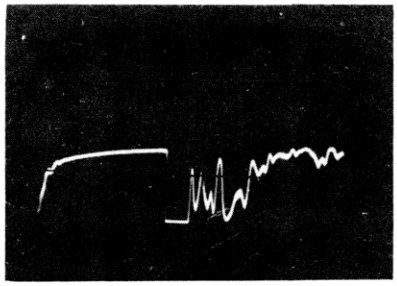

Brass (70-30)
1-in. cube
f = 16.9 Mc/sec
pulse width = 3.7 μsec
sweep = 122 μsec

(c)

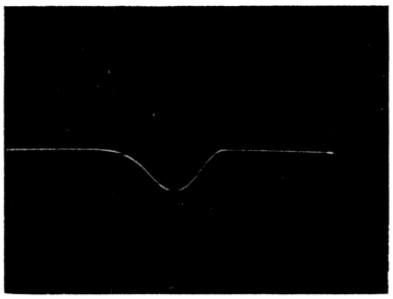

Magnesium
diam. = 1 in.
length = 1 1/4 in.
D* = 0.35 mm
f = 28.2 Mc/sec
pulse width = 2.5 μsec
sweep = 12.2 μsec
D/λ = 2.5

D* = grain size

(d)

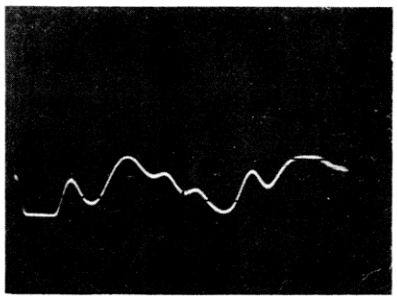

Aluminum
diam. = 3/4 in.
length = 1½ in.
D = 0.21 mm
f = 28.2 Mc/sec
pulse width = 2.5 μsec
sweep = 24.4 μsec
D/λ = 1.5

Figure 3.

of the interference processes, producing altered patterns. Similar variations occur for the same reason if the frequency or alignment of the sample is changed slightly.

Figure 3c is a view of a single pulse displayed on an expanded sweep in proper position for determining its amplitude and time elapsed with respect to the start of the sweep. No pulse distortion is evident since fine-grained magnesium was used. Figure 3d is a similar view of fine-grained aluminum showing considerable pulse distortion. No measurements can be made with such a pulse.

Attenuation. The results of measurements made on two representative magnesium specimens for different frequencies are plotted in Figs. 4 and 5. The former, for a fine-grained sample,

appears to be homogeneous since the points on the logarithmic plots lie along straight lines corresponding to time exponentials on the cathode-ray tube screen The latter, for a coarse-grained sample shows much scatter indicating departure from an exponential resulting from the large grains The attenuation of the first sample can be measured accurately, whereas considerable error could be introduced in the second case These curves are typical of both the good and bad experimental runs for magnesium and aluminum

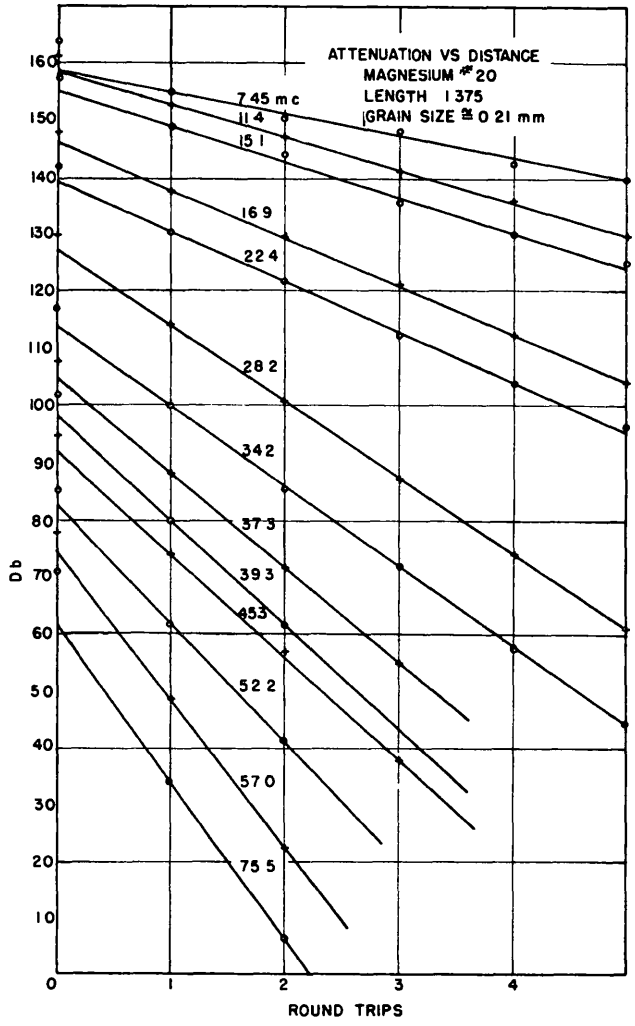

Figure 4

From the slope of these curves, and the power reflection loss at the water-metal interface (see below), graphs of attenuation in the metal vs frequency for different grain size can be plotted Figure 6 illustrates such curves for the two samples used above Although the large scatter about the mean is disturbing, this is the nature of the processes under investigation, and cannot be avoided The linear variation of attenuation with frequency should be noted For grain sizes lying between the two cases shown, straight lines are also found but the slopes assume values intermediate to those shown

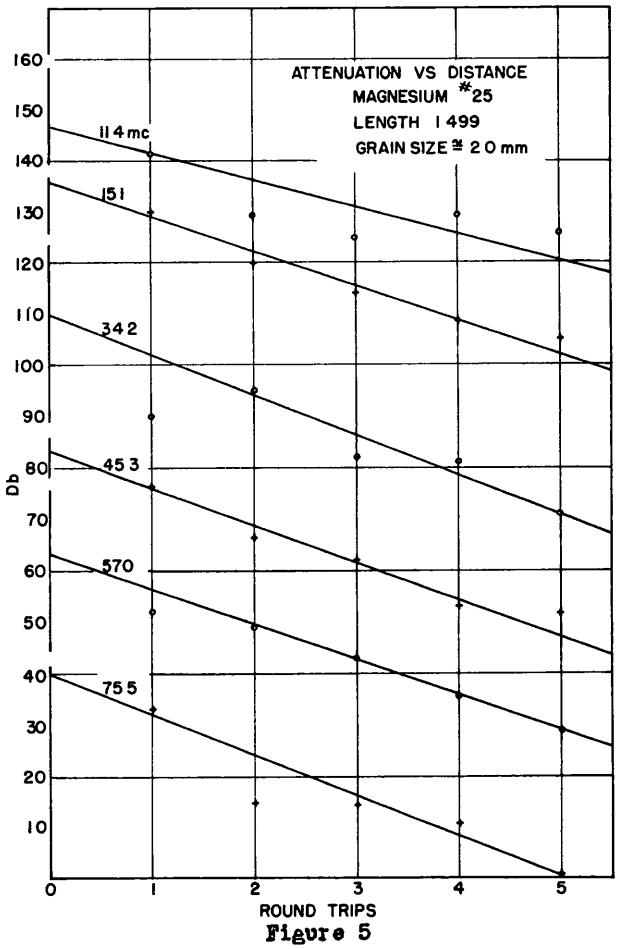

Figure 5

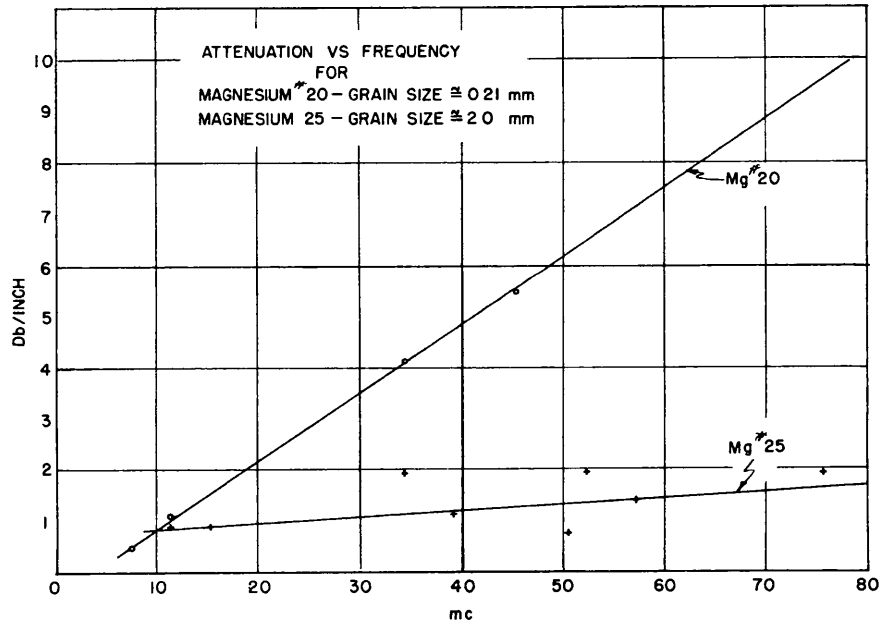

Figure 6

Figure 7, is a plot of the slopes of the previous curves as functions of grain size The attenuation α is stated in terms of the power absorption coefficient rather than in decibels per inch where α is defined from the relation

$$I = I_o e^{-2\alpha x}$$

where I = intensity in a plane wave at point x

I_o = intensity in a plane wave at point $x = 0$

α = amplitude absorption coefficient

The solid rectangles indicate the area of error for the experimental results with magnesium, and the dotted rectangles indicate the same for aluminum. Although these areas are large, more information can be obtained from these data than is at first thought possible

Even if a larger per cent error in grain size for the uppermost point were assumed, the actual grain size limits would not be increased substantially Similarly, a larger per cent error in absorption per cycle for the point farthest to the right would

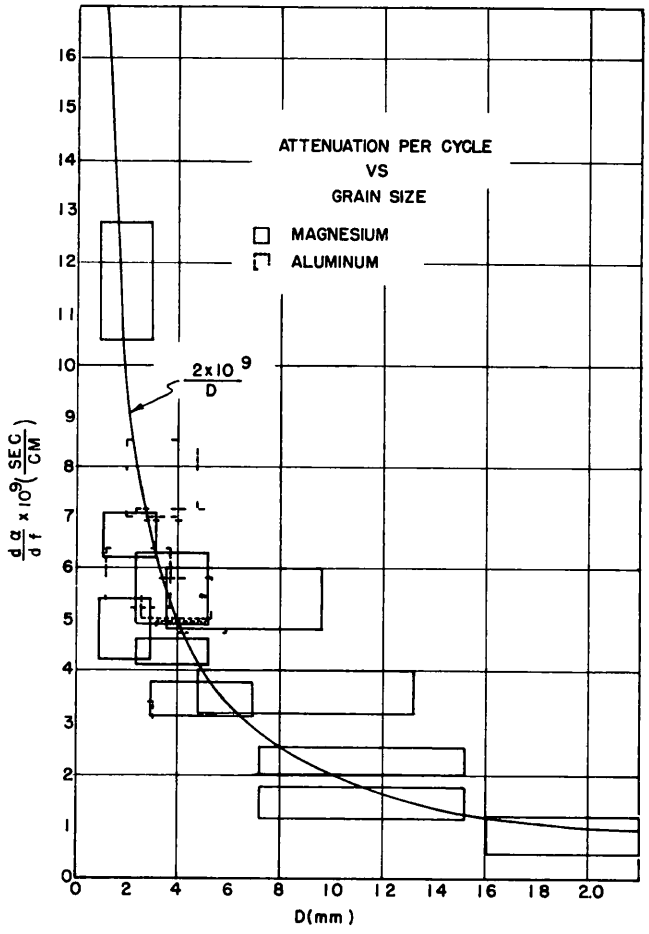

Figure 7

not increase the height of this rectangle greatly Therefore the extreme limits of the curve eventually drawn are rather well defined If we now consider the number of curves that will also pass through the center of distribution of the remaining points our choice is severely limited The solid curve finally drawn is an equilateral hyperbola which gives

$$\frac{d\alpha}{df} = \frac{2\times10^{-9}}{D}$$

or

$$\alpha = 2\times10^{-9}\,\frac{f}{D} + K(D)\ \text{cm}^{-1}$$

f = frequency in cycles/sec

D = grain size in mm

$K(D)$ = a function independent of frequency but possibly dependent on D, in cm^{-1}

$K(D)$ is the value of α for either $f = 0$ or $D = \infty$; neither of which were obtained in these experiments By extrapolating the attenuation vs frequency curves to $f = 0$, however, for all the metals tested $K(D)$ lies in the region between $\pm$ 05 cm^{-1}

Velocity The velocity of propagation of longitudinal waves in infinite plates is given by

$$V^2 = \frac{E(1-\sigma)}{\rho(1+\sigma)(1-2\sigma)} \qquad (1)$$

ρ = density

E = Young's modulus

σ = Poisson's ratio

This velocity is measured experimentally by dividing twice the sample length by the time difference between successive echoes With the known constants for the polycrystalline metal in question, Eq (1) can be used to check the experimental value This was done for aluminum and is recorded below.

For magnesium, no consistent information for the polycrystalline metal could be found, so the results of calculations made for a single crystal were used The velocity for a polycrystalline sample represnets a weighted average of all values present in the individual crystal These are also tabulated below. The agreement in both cases is very good and no velocity dispersion was measured

Metal	Observed V (in units of 10^5 cm/sec)	Calculated V_5 (in units of 10^5 cm/sec)	Source of elastic constants
Mg	5.77 $\pm$ .004	5 70 - 5 81 (for single crystal)	R F S Hearmon, Rev Mod Phys. 18,(3) July, 1946, p.409
Al	6.31 $\pm$ .01	6 32	G W C Kaye and T H.Laby "Table of Phys and Chem Constants",Longman, Green 1941

Power Reflection Coefficient. The power reflection coefficient at the interface between two semi-infinite media is given in the usual way by

$$R = \left(\frac{\rho_1 V_1 - \rho_2 V_2}{\rho_1 V_1 + \rho_2 V_2}\right)^2 \qquad (2)$$

where ρ= density, V = velocity, and the subscripts refer to the respective media. Experimental determination of this quantity was performed by making two absorption-distance runs on each sample The metal was completely immersed in water in one case but only one surface was immersed in the other case Since the reflection at an air-to-metal boundary is essentially unity, the difference in the attenuation in the two cases equals the reflection loss at one metal-water interface or $-10 \log_{10} R$ Curves of these runs for the two magnesium specimens previously discussed are shown in Fig 8 The vertical displacement between corresponding points of the two curves in each set equals n x $10 \log_{10} R$, where n is the order of the round trip From this measured reflection loss,

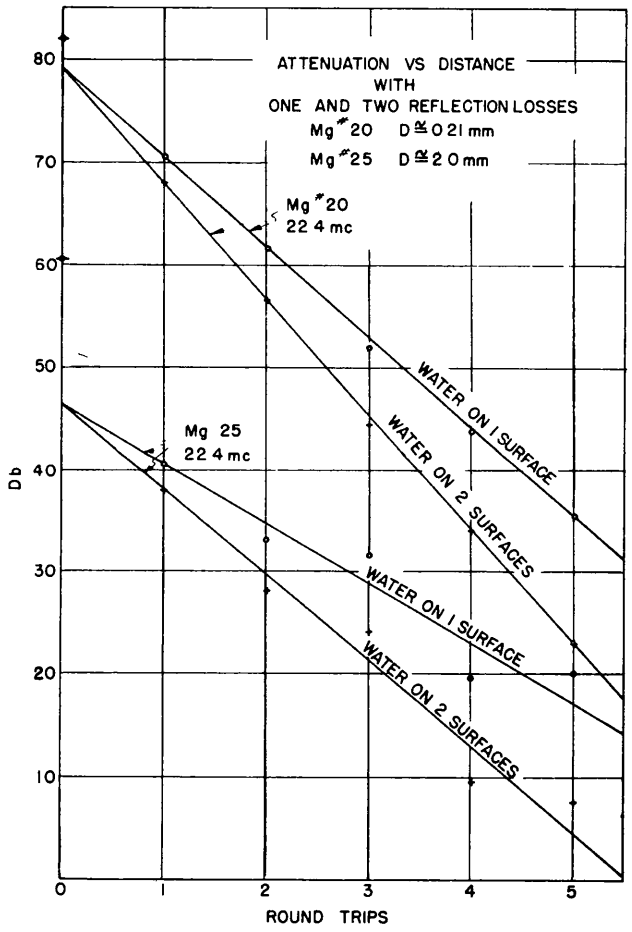

Figure 8

R was determined for each metal and checked against the value calculated from Eq (2) The constants for water were taken from A B Wood, "Textbook of Sound" The results are

Metal	R Observed	R Calculated
Mg	0 558	0 561
Al	0 708	0 714

and again the agreement is excellent

It should be noted that this applies only for propagation from the metal to the water and not in the opposite direction When propagating into the metal, standing waves are set up at the surface due to the inhomogeneities, and the conditions for application of Eq (2) are not present This discrepancy was observed The departure occurs at a lower frequency for larger grains, because the non-homogeneities appear at a lower frequency

Quality of Pulse Transmission. The pulse transmission properties of metals attenuation and distortion are determined by the degree of isotropy of the single crystals Isotropic solids, even though they may be polycrystalline would show little scattering and hence, little absorption since the grain boundaries present no discontinuity to the incident wave The degree of isotropy is suggested as a figure of merit to evaluate the pulse transmission properties of polycrystalline solids

The strains in any solid can be expressed in terms of the stress if the elastic moduli matrix for the solid is known. The only difference between the cubic matrix and the isotropic matrix is that in the former case $S_{44} \neq 2(S_{11} - S_{12})$ where S_{ik} are the elements of the matrices The hexagonal matrix has the additional inequalities, $S_{13} \neq S_{12}$ and $S_{33} \neq S_{11}$ If the substance were isotropic, these respective inequalities would not exist, hence this departure can be used as a figure of merit The following tables list all cubic and hexagonal metals whose constants are given by Hearmon[1], and the departure of the listed values from unity is a measure of the anisotropy The observed results agree with these predictions as noted below Tungsten is the only outstanding example of an isotropic polycrystalline solid It should transmit pulses with little scattering even at high ultrasonic frequencies

1 R F S Hearmon, "Elastic Constants of Anistropic Materials" Rev Mod Phys 18, (3) July 1946 p 409

Cubic System Alloys

Metal	$\frac{S_{44}}{2(S_{11} - S_{12})}$	Predicted Pulse Transmission
Cu_3Au	40	fair
72%Cu, 28%Zn	25	poor (observed)
β--Brass(CuZn)	05	very poor
5%Cu, 95%Al	85	good
75%Ag, 25%Au	.35	fair
50%Ag, 50%Au	35	fair
25%Ag, 75%Au	35	fair

Cubic System Elements

Metal	$\frac{S_{44}}{2(S_{11} - S_{12})}$	Predicted Pulse Transmission
Al	81	good (observed)
Cu	31	poor (observed)
Au	35	fair
Fe	.42	fair
Pb	26	poor
K	.16	poor
Ag	.35	fair
Na	14	poor
W	1 0	excellent

Hexagonal System Elements (5 coefficients)

Metal	$\frac{S_{13}}{S_{12}}$	$\frac{S_{33}}{S_{11}}$	$\frac{S_{44}}{2(S_{11}-S_{12})}$	Predicted Pulse Transmission
Cd	6.2	2.9	2.1	fair
Mg	.58	.89	.99	very good (observed)
Zn	-11.5	3 4	1 7	fair